CORTEX 63 (2015) 79–89

Available online at www.sciencedirect.com

ScienceDirect

Journal homepage: www.elsevier.com/locate/cortex

Clinical neuroanatomy

Common molecular basis of the sentence comprehension network revealed by neurotransmitter receptor fingerprints

Karl Zilles [a,b,*,1], Maraike Bacha-Trams [a,c,1], Nicola Palomero-Gallagher [a], Katrin Amunts [a,d] and Angela D. Friederici [c]

[a] Institute of Neuroscience and Medicine (INM-1), Research Centre Juelich, Germany
[b] Department of Psychiatry, Psychotherapy, and Psychosomatics, University Hospital Aachen, RWTH Aachen University, Germany
[c] Max Planck Institute for Human Cognitive and Brain Sciences, Department of Neuropsychology, Leipzig, Germany
[d] C. & O. Vogt Institute for Brain Research, Heinrich-Heine-University Duesseldorf, Germany

ARTICLE INFO

Article history:
Received 13 February 2014
Reviewed 4 April 2014
Revised 2 June 2014
Accepted 10 July 2014
Action editor Marco Catani
Published online 12 August 2014

Keywords:
Language
Transmitter receptors
Brain mapping
Human cerebral cortex

ABSTRACT

The language network is a well-defined large-scale neural network of anatomically and functionally interacting cortical areas. The successful language process requires the transmission of information between these areas. Since neurotransmitter receptors are key molecules of information processing, we hypothesized that cortical areas which are part of the same functional language network may show highly similar multireceptor expression pattern ("receptor fingerprint"), whereas those that are not part of this network should have different fingerprints. Here we demonstrate that the relation between the densities of 15 different excitatory, inhibitory and modulatory receptors in eight language-related areas are highly similar and differ considerably from those of 18 other brain regions not directly involved in language processing. Thus, the fingerprints of all cortical areas underlying a large-scale cognitive domain such as language is a characteristic, functionally relevant feature of this network and an important prerequisite for the underlying neuronal processes of language functions.

© 2014 Elsevier Ltd. All rights reserved.

1. Introduction

Recent functional neuroimaging studies on language (Friederici, 2011; Vigneau et al., 2006) investigating syntactic, semantic and verbal working memory processes identified circumscribed activations located within the two classical language regions, i.e., Broca's region in the inferior frontal gyrus (IFG) and Wernicke's region in the superior temporal

* *Corresponding author*. Institute of Neuroscience and Medicine (INM-1), Wilhelm Johnen Str., 52425 Jülich, Germany.
E-mail addresses: k.zilles@fz-juelich.de (K. Zilles), mareike.bacha-trams@aalto.fi (M. Bacha-Trams), n.palomero-gallagher@fz-juelich.de (N. Palomero-Gallagher), k.amunts@fz-juelich.de (K. Amunts), friederici@cbs.mpg.de (A.D. Friederici).
[1] Authors contributed equally to the manuscript.
http://dx.doi.org/10.1016/j.cortex.2014.07.007
0010-9452/© 2014 Elsevier Ltd. All rights reserved.

gyrus. Within Broca's area the dorsal part of the left pars opercularis (44d) processes hierarchically structured syntax (e.g., center-embedded relative clauses), whereas the left inferior frontal sulcus at the junction with the precentral sulcus (IFS1/IFJ) is involved in syntactic verbal working memory (Makuuchi, Bahlmann, Anwander, & Friederici, 2009). An involvement of 44d was also reported for the processing of complex sentences in other studies (Friederici, Fiebach, Schlesewsky, Bornkessel, & von Cramon, 2006; Grewe et al., 2005). The pars triangularis within Broca's area, which was subdivided into a more posterior part (45p) and a more anterior part (45a) (Amunts et al., 2010), is involved in processing semantic aspects both at the word (Fiez, 1997; Heim et al., 2009; Thompson-Schill, D'Esposito, Aguirre, & Farah, 1997) and sentence levels (Newman, Ikuta, & Burns, 2010) as well as for sentence comprehension in general (Saur et al., 2008). The posterior superior temporal gyrus and sulcus (pSTG/STS) play a significant role in sentence processing (Friederici, Makuuchi, & Bahlmann, 2009), and in the brain-based decoding of human voice and speech (Formisano, De Martino, Bonte, & Goebel, 2008). These different regions of the inferior frontal and temporal cortex are known to be structurally connected by short-range connections (Makuuchi et al., 2009; Upadhyay et al., 2008) and by long-range fiber bundles (Catani, Jones, & ffytche, 2005; Friederici et al., 2006; Saur et al., 2008). Thereby the different areas constitute a large-scale fronto-temporal language network for sentence comprehension (Friederici, 2009, 2011).

Neurotransmitters and their receptors are key molecules of neuronal function. Within a given brain region, different receptor types are expressed at largely varying densities. Thus, the balance between the densities of different receptors in a single brain region, and not the mere presence or absence of a single receptor type, results in a regional specific receptor pattern, i.e., a "receptor fingerprint" (Zilles et al., 2002). Consequently, receptor fingerprints represent the molecular default organization of the regionally specific local information processing in each cortical area. Differences between the fingerprints of unimodal sensory, motor, and multimodal association areas of the human cerebral cortex (Caspers, Schleicher, et al., 2013; Eickhoff, Rottschy, Kujovic, Palomero-Gallagher, & Zilles, 2008; Zilles, Palomero-Gallagher, & Schleicher, 2004) underlined the regional diversity of multireceptor expression levels. E.g., cortical areas belonging either to the dorsal or ventral visual streams have similar fingerprints within each of the streams, but differ between streams (Eickhoff et al., 2008). Connectionally distinct areas within inferior parietal lobule (IPL) also differ in their receptor fingerprints (Caspers, Schleicher, et al., 2013). Since the cortical areas of the dorsal or ventral streams, as well as those of the inferior parietal cortex are immediate neighbors, it could be argued, that the similarities in receptor fingerprints resulted merely from the close spatial relation of areas within each of the three regions, and not from their common affiliation to a given functional system. It is currently not known, whether widely distributed areas of the same cognitive network have similar fingerprints despite of their spatial distance. Therefore, we here investigated whether areas belonging to the large-scale fronto-temporal language network for sentence comprehension differ in their receptor fingerprints or share a common multireceptor expression, despite the fact that the areas are widely distributed between the temporal and frontal lobes. In each of these areas, multiple excitatory, inhibitory and modulatory transmitter receptors subserve the local computational processes. Here we hypothesized, that areas constituting the fronto-temporal language network may not only be characterized by similar receptor fingerprints, but also that their fingerprints differ from those of areas subserving non-language functions, i.e., different unimodal sensory, motor or multimodal functions.

2. Material and methods

Brain regions were examined in the left and right hemispheres of brains obtained from individuals (two males and two females; 77 ± 2 years of age) with no clinical records of neurological or psychiatric disorders, who participated in the body donor program of the Department of Anatomy, University of Düsseldorf. Causes of death were pulmonary edema, multiorgan failure, bronchial cancer, or sudden cardiac death.

Brains were removed from the skull within 24 h after death. Each hemisphere was dissected into five or six slabs in the coronal plane (25–30 mm thickness), frozen in isopentane at −40 °C and stored at −70 °C. Using a large-scale cryostat microtome, each slab comprising a coronal section through the complete human hemisphere was cut into continuous series of coronal sections (20 μm thickness), which were thaw-mounted onto glass slides.

2.1. *Brain regions*

Cortical areas studied here could be divided into two major groups, i.e., areas involved in language, particularly in sentence comprehension, and "non-language" related areas, which do not belong to this fronto-temporal language network.

2.1.1. *Language-related areas*

Three regions (44d, IFS1/IFJ, and pSTG/STS, Fig. 1A) were functionally (IFS1/IFJ, pSTG/STS; Friederici et al., 2006, 2009; Grewe et al., 2005; Makuuchi et al., 2009) and additionally receptor architectonically (44d; Amunts et al., 2010) defined. These three regions were found to be activated during processing of syntactically complex, embedded sentences (Friederici et al., 2009; Makuuchi et al., 2009). An involvement of 44d was also reported for the processing of non-canonical object first sentences (Friederici et al., 2006; Grewe et al., 2005). These regions were localized in the postmortem brains using their characteristic anatomical landmarks (i.e., sulci and gyri). Five further language-related regions (44v, 45a, 45p, 47 and Te2, Fig. 1A) were defined based on cyto- and receptor architectonical criteria. Area 44v is the ventral part of the left pars opercularis of Broca's region, and can be architectonically segregated from its dorsal counterpart 44d and from the rostrally adjoining area 45 (Amunts et al., 2010, 1999). Areas 45a and 45p (Amunts et al., 2010) were included as the complete region has been reported to be activated during processing of semantic aspects at both the word (Fiez, 1997; Heim et al., 2009; Thompson-Schill et al., 1997) and the

sentence level (Newman et al., 2010). Area 47 can be localized cytoarchitectonically (Brodmann, 1909) and by its position ventral to 45a and 45p, from which it is separated by the horizontal branch of the lateral fissure (Fig. 1A). Functional studies have demonstrated its involvement in language comprehension (Dronkers, Wilkins, Van Valin, Redfern, & Jaeger, 2004; Turken & Dronkers, 2011). The temporal area Te2 was defined cyto- and receptor architectonically (Morosan, Schleicher, Amunts, & Zilles, 2005), and its function in speech stimuli and language processing was reported (Amunts et al., 2010; Kubanek, Brunner, Gunduz, Poeppel, & Schalk, 2013; Morosan et al., 2005).

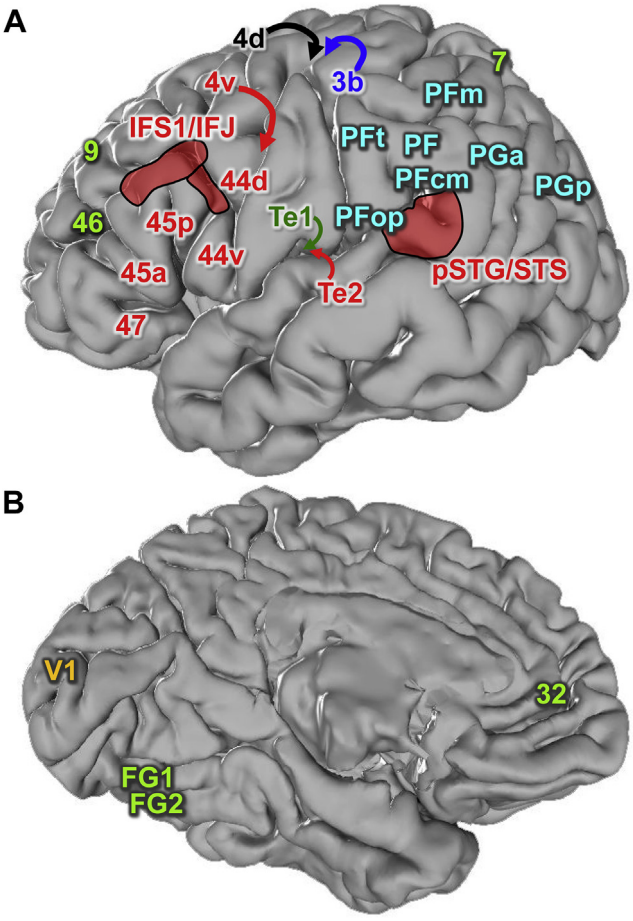

Fig. 1 – Localization of examined cortical regions. Localization of examined cortical regions projected on the lateral (A) and medial (B) surfaces of the single subject MNI template brain (Evans et al., 2012): 3b (primary somatosensory cortex, part of BA 3); 4 (primary motor cortex); 7 (BA 7); 9 (BA 9); 32 (BA 32); 44d (dorsal BA 44); 44v (ventral BA 44); 45a (anterior BA 45); 45p (posterior BA 45); 46 (BA 46); 47 (BA 47); FG1 and FG2 (cytoarchitectonically defined extrastriate visual areas on the fusiform gyrus); IFS1/IFJ (areas in the inferior frontal sulcus and at the junction between the inferior frontal and precentral sulci); PF, PFm, PFcm, PFop and PFt (areas located within BA40); PGa and PGp (areas located within BA 39); pSTG/STS (areas of the posterior superior temporal gyrus and sulcus); Te1 (primary auditory cortex, BA 41); Te2 (auditory belt area, BA 42); V1 (primary visual cortex, BA 17). BA: Brodmann areas (Brodmann, 1909). Red indicates language-related brain regions with similar fingerprints (see Fig. 4). Dark blue, dark green, yellow and black encode the primary somatosensory, auditory and visual cortices, and the hand representation region of the motor cortex, respectively. Light blue encodes IPL areas, whereas light green represents prefrontal, superior parietal, cingulate, and extrastriate fusiform areas.

2.1.2. *Non-language related areas*

Eighteen cyto- and/or receptor architectonically localizable cortical areas, which are not associated with sentence comprehension, were included in order to compare the multireceptor expression of language-related versus that of non-language related areas (Fig. 1A and B): primary auditory cortex Te1 (Morosan et al., 2005), hand (4d) and mouth (4v) representation regions within the primary motor area 4 (Geyer et al., 1996), primary visual area V1 (Amunts, Malikovic, Mohlberg, Schormann, & Zilles, 2000; Eickhoff, Rottschy, & Zilles, 2007), extrastriate higher visual areas FG1 and FG2 on the fusiform gyrus (Caspers, Zilles, Amunts, et al., 2013, Caspers, Zilles, Eickhoff, et al., 2013), primary somatosensory area 3b (Geyer, Schleicher, & Zilles, 1997), prefrontal areas 9 and 46 (Brodmann, 1909), area 7 of the superior parietal lobule (Scheperjans, Palomero-Gallagher, Grefkes, Schleicher, & Zilles, 2005), areas PF, PFcm, PFm, PFop, PFt, PGa, and PGp of the IPL(Caspers, Schleicher, et al., 2013), and cingulate area 32 (Palomero-Gallagher et al., 2009). These areas are mainly involved in motor control, visual and somatosensory perception, higher visual functions, and various cognitive or emotion-related functions (Caspers, Zilles, Amunts, et al., 2013, Caspers, Zilles, Eickhoff, et al., 2013, Caspers, Zilles, Laird, & Eickhoff, 2010; Corbetta, Patel, & Shulman, 2008; Eickhoff et al., 2007; George et al., 1995; Jakobs et al., 2009; Keysers & Gazzola, 2009; Kross, Davidson, Weber, & Ochsner, 2009; Smith et al., 2011).

2.2. *Experimental procedure*

The regional distribution of 15 different neurotransmitter receptor binding sites (AMPA, kainate, NMDA, $GABA_A$, $GABA_B$, benzodiazepine binding sites of the $GABA_A$ receptor (BZ), M_1, M_2, M_3, nicotinic α_4/β_2, α_1, α_2, 5-HT_{1A}, 5-HT_2, D_1) for glutamate, γ-amino butyric acid (GABA), acetylcholine, noradrenaline, serotonin and dopamine were visualized, and their concentrations [fmol/mg protein] were measured in 26 brain regions of four left and four right human hemispheres by means of quantitative *in vitro* receptor autoradiography (Zilles, Schleicher, Palomero-Gallagher, Amunts, 2002). These receptor types were selected because they occur at relatively high concentrations in all regions of the cerebral cortex, and have been proven to contribute considerably to the segregation of cortical areas based on regional and laminar expression patterns (Caspers, Schleicher, et al., 2013; Eickhoff et al., 2008; Palomero-Gallagher et al., 2009; Zilles, Palomero-Gallagher, et al., 2002, Zilles et al., 2004).

Autoradiographic labeling of the sections with tritium [^{3}H]-labeled ligands was performed according to standardized protocols (Zilles, Schleicher, et al., 2002; Supplementary Table 1). The experimental procedure included three successional

steps: 1) Pre-incubation to rehydrate the tissue and remove endogenous ligands and other substances which potentially bind to the receptors. 2) Main incubation to label the receptors with only the respective tritiated ligands in nM, or with the tritiated ligands in presence of the respective non-labeled competitors in μM. By comparing these two experimental conditions, the specific binding could be calculated: The incubation with only the tritiated ligand denoted the total binding, whereas the incubation with the additional non-labeled competitor showed the non-specific binding. The specific binding was calculated as the difference between total binding and non-specific binding. It was less than 5% in all cases. 3) Final rinsing to stop binding and remove superfluous radioactive ligands.

Radioactively labeled sections were co-exposed with [^{3}H]-plastic scales of known radioactivity against [^{3}H]-sensitive films for 4–18 weeks. The developed films were digitized using a CCD-camera.

2.3. *Densitometric analysis*

Gray values of the digitized images were transformed into radioactivity concentrations by a non-linear transformation computed from the gray values of the co-exposed plastic standards of known radioactivity concentrations. These linearized autoradiographs were contrast enhanced, and color coded in a spectral color sequence for a better visualization of regional differences.

Regions of interest were selected and defined using cyto- and receptor architectonical as well as landmark-based identification as described in the literature (Amunts et al., 2010, 1999; Brodmann, 1909; Caspers, Schleicher, et al., 2013; Caspers, Zilles, Eickhoff, et al., 2013, Eickhoff et al., 2007; Friederici et al., 2009; Geyer et al., 1997; Makuuchi et al., 2009; Morosan et al., 2005; Palomero-Gallagher et al., 2009; Scheperjans et al., 2005; Zilles & Amunts, 2010). Receptor densities were extracted from the regions of interest based on a previously described densitometric analysis (Zilles, Schleicher, et al., 2002). For each of the examined receptor types, profiles oriented vertically to the cortical surface and covering the full cortical width were extracted from the linearized autoradiographs (Zilles, Schleicher, et al., 2002). The area below the profile quantifies the mean areal density in fmol/mg protein. Densities were averaged over three sections and four hemispheres, and provided the mean value for each receptor in each area. These values were registered for each area separately in a polar plot. The resulting graph is the receptor fingerprint of each area. It allows the visualization of the densities of multiple receptors within and between different cortical regions. For subsequent statistical analyses, the mean densities of each region were normalized to the grand mean over all examined regions for each receptor separately.

2.4. *Statistical analysis*

The degree of (dis)similarity between receptor fingerprints was determined by means of multivariate statistical analyses in which the receptor fingerprints of each area were treated as feature vectors describing their multi-receptor balance (Palomero-Gallagher et al., 2009). A hierarchical cluster analysis (Euclidean distances and Ward linkage) describes groupings of regions according to the degree of similarity of their receptor architecture. Thus, the smaller the Euclidean distance between two ROIs, the greater the similarity in shape and size of their fingerprints. Regions within a cluster have a similar balance between receptors, which is different from that of regions in other clusters. Additionally, a multidimensional scaling analysis was performed to reduce the 15-dimensional space (15 different receptor types) into two dimensions for graphical representation of the Euclidean distances between cortical regions.

A discriminant analysis was carried out to determine which receptor types contributed most and which least, to the grouping of areas revealed by the hierarchical cluster analysis.

3. Results and discussion

Quantitative analysis of the densities of the different excitatory, inhibitory and modulatory receptors revealed a variation by two orders of magnitude in the examined brain regions. The laminar distribution of the various receptor types in the left hemisphere is exemplarily shown in color coded images of eight of the 26 examined cortical regions (Fig. 2). Most receptors are present in highest densities in the supragranular layers, with the notable exception of the glutamatergic kainate receptors, which reach the highest densities in the infragranular layers. Within a given receptor type, laminar distribution patterns varied to different degrees between cortical areas. For example, layer IV of the primary visual cortex (V1) differs from that of the language-related areas by its extremely low kainate, $GABA_B$, and α_1 receptor densities in its sublayers IVb and IVc, but high α_2 receptor densities in its sublayer IVa. Furthermore, higher NMDA, $GABA_A$ receptor densities are found in sublayer IVc of V1 than in contrast to layer IV of the language areas. Area V1 is also characterized by an extremely high M_2 receptor density throughout all cortical layers and a very high M_3 receptor density in supragranular layers when compared with the language-related areas 44d, 45, IFS1/IFJ, and pSTG/STS (Fig. 2).

The variety of multireceptor expression in the different cortical areas can be visualized by receptor fingerprints (Zilles, Palomero-Gallagher, et al., 2002; Zilles, Schleicher, et al., 2002). The fingerprints of the left hemisphere (Fig. 3) show similarities and dissimilarities between the 26 regions. Although the emphasis of the present study is on the left hemisphere, because the functional imaging data of the language comprehension studies revealed left-lateralized activations in areas 44d, IFS1/IFJ and pSTG/STS (Friederici et al., 2006, 2009; Grewe et al., 2005; Makuuchi et al., 2009), we also acquired data from the right hemisphere (Fig. S1).

The similarities or differences of the multireceptor fingerprints between all 26 areas were analyzed using hierarchical cluster and multidimensional scaling analyses separately for data obtained from the left and right hemispheres (Fig. 4 and Fig. S2). The cluster analysis of receptor densities measured in the left hemisphere demonstrates that areas 44v, 44d, 47, 45a, 45p, IFS1/IFG, pSTG/STS, 47 and Te2 cluster together and have similar receptor fingerprints, which differ from those of the

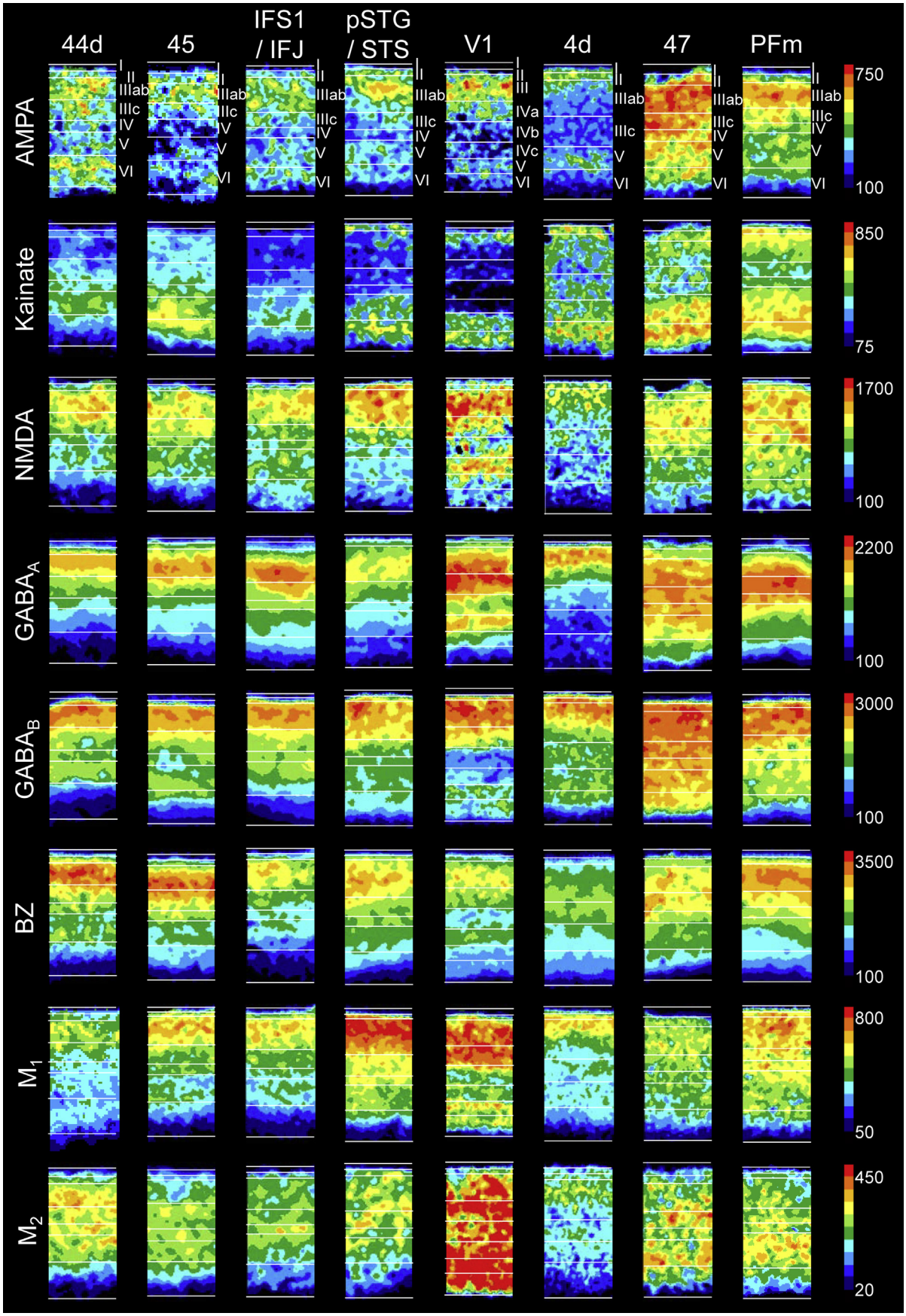

Fig. 2 – Laminar distribution of receptors in selected cortical areas. Color coded receptor autoradiographs visualizing the laminar distribution of glutamate (AMPA, kainate, NMDA), GABA (GABA$_A$, GABA$_B$, GABA$_A$ associated benzodiazepine (BZ) binding sites), acetylcholine (M$_1$, M$_2$, M$_3$, nicotinic α_4/β_2), norepinephrine (α_1, α_2), serotonin (5-HT$_{1A}$, 5-HT$_2$) and dopamine (D$_1$) receptors in 8 of the 26 examined brain areas. Color coding indicates receptor densities in fmol/mg protein.

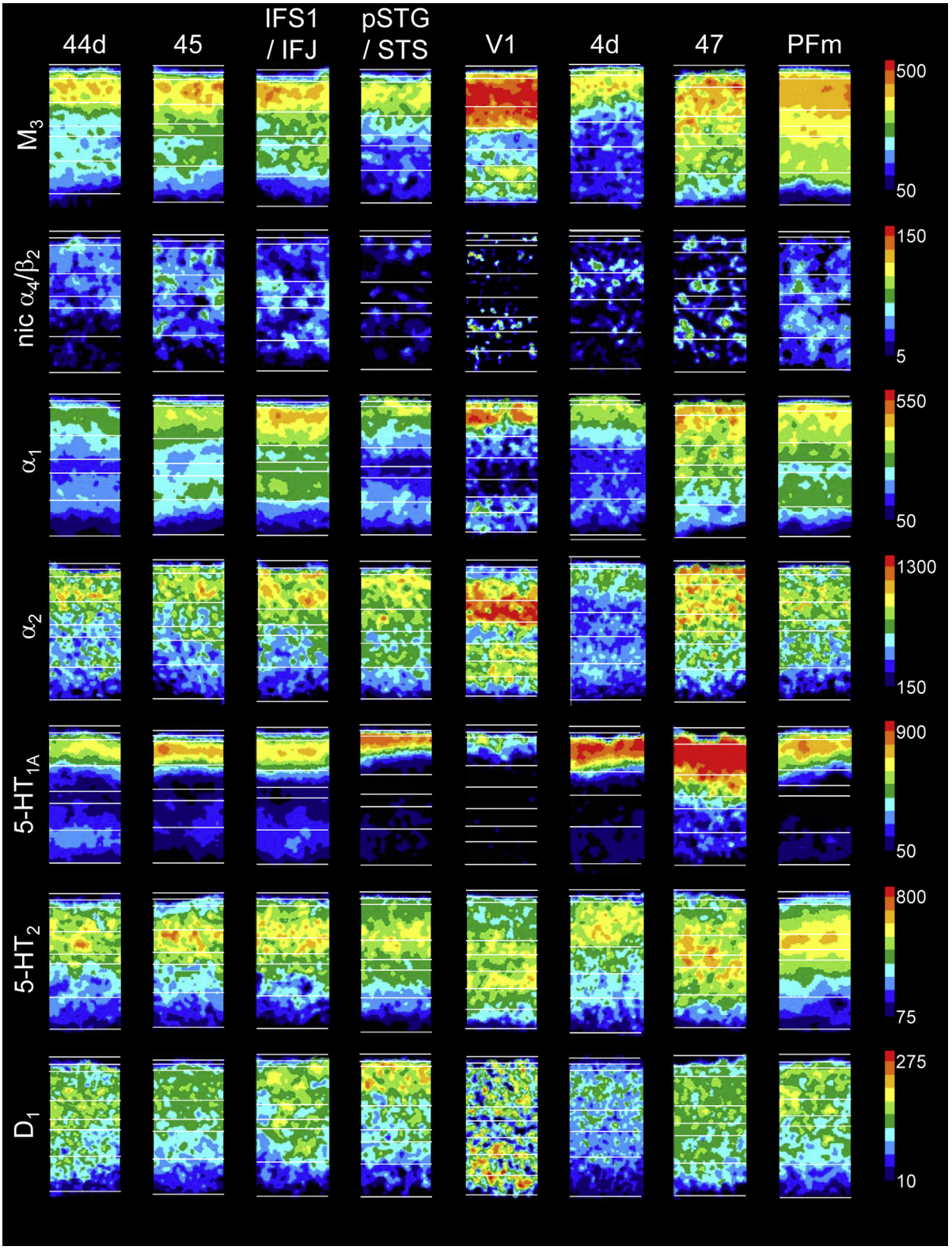

Fig. 2 – (*continued*).

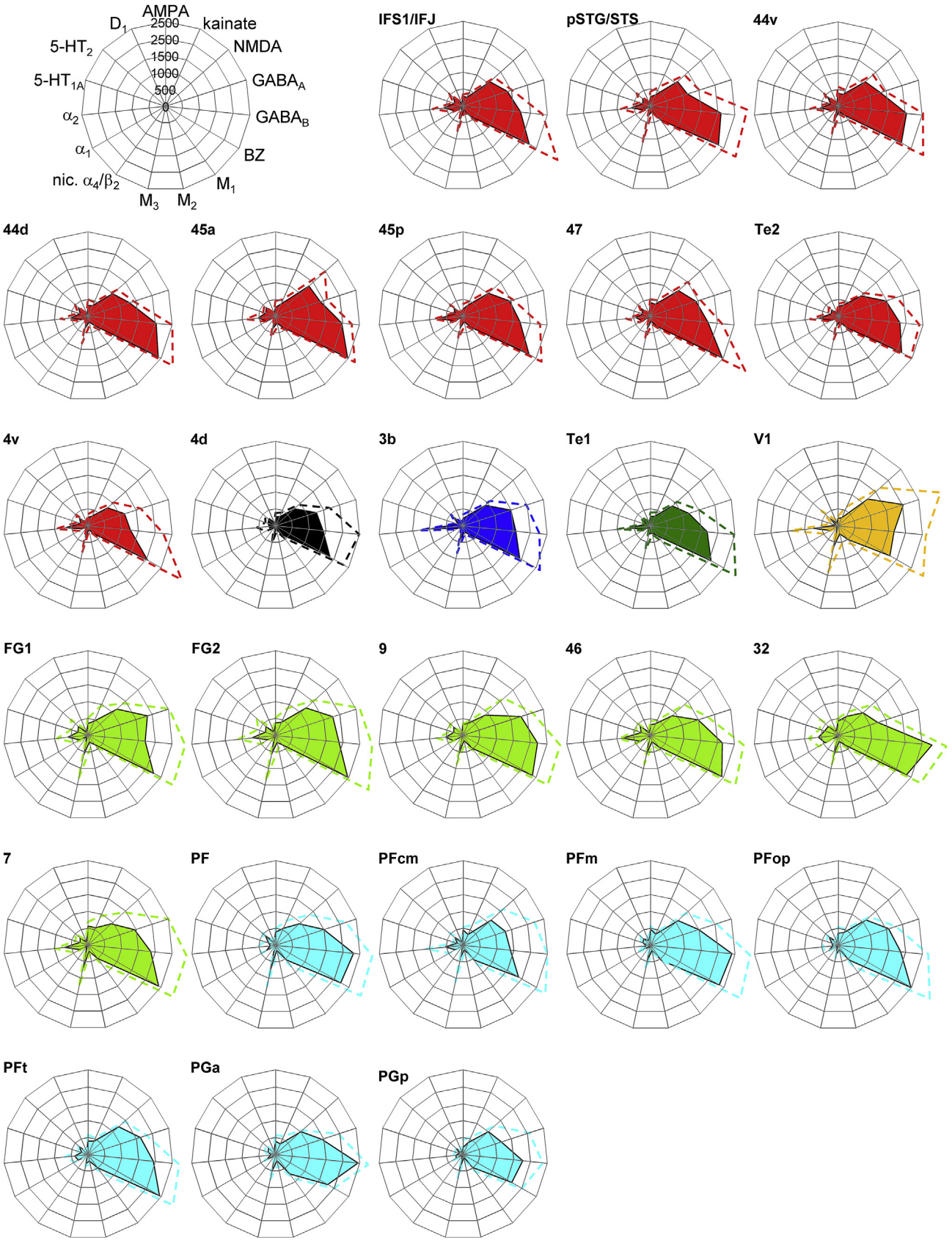

Fig. 3 – Receptor fingerprints of the examined brain regions in the left hemisphere. Absolute densities (in fmol/mg protein) of 15 receptors shown as fingerprints of the 26 examined brain regions. The positions of the different receptor types and the axis scaling are identical in all polar plots, and specified in the polar plot at the top left corner of the figure. The colored area represents the mean absolute receptor densities; SEM is given by the dashed lines. Color coding as in Figs. 1, 4A and B.

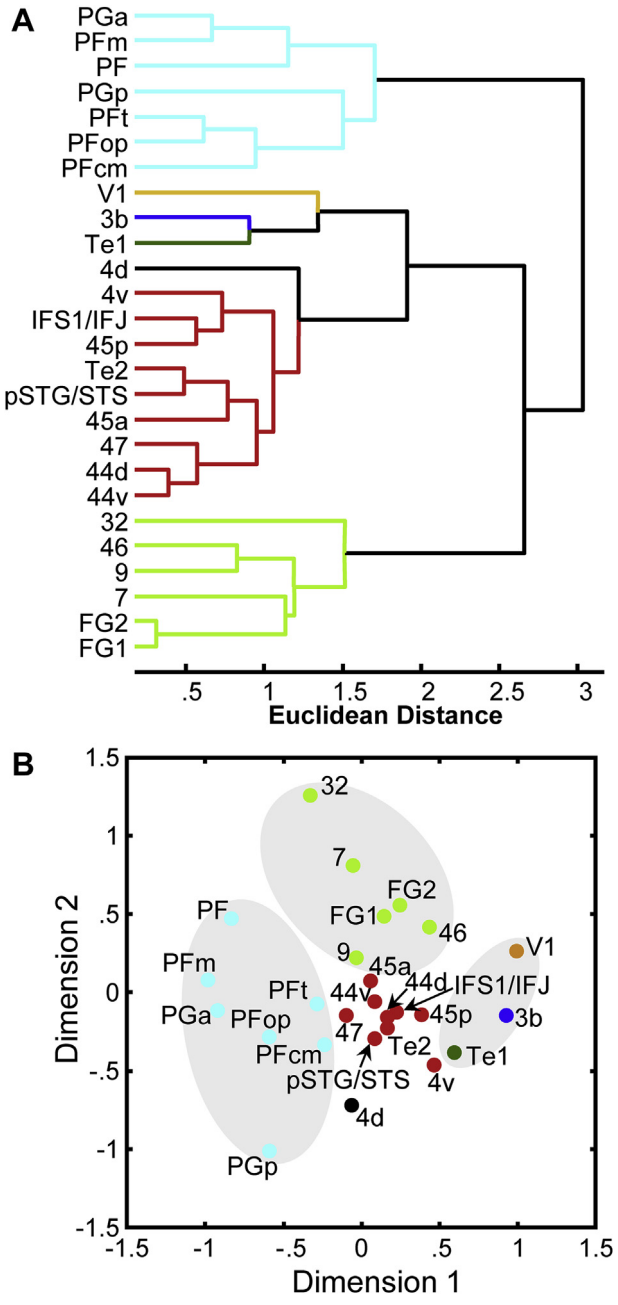

Fig. 4 – Hierarchical cluster tree and multidimensional scaling of receptor fingerprints in 26 cortical brain regions. (A) Hierarchical cluster tree of receptor distribution patterns in the left hemisphere. (B) Multidimensional scaling resulting in a 2D display of the 15-dimensional receptor feature vectors of the receptor fingerprints of 26 cortical regions measured in the left hemisphere.

three primary sensory areas (V1, 3b, and Te1), particularly concerning the 5-HT_{1A}, M_2 and kainate receptors, as revealed by the discriminant analysis. Interestingly, a separate analysis of the mouth (4v) and hand (4d) representation regions within the primary motor cortex revealed a closer relationship of area 4v than of area 4d to the language-related areas (Fig. 4A). The language-related regions (all regions coded in red in Fig. 1) in addition to the three regions that were functionally defined to support the processing of syntactically complex sentences (44d, IFS1/IFJ, pSTG/STS in Fig. 1) certainly contribute to language processing. The three syntax-related regions were defined by subtracting activation for syntactically simple sentences from syntactically complex sentences (Friederici et al., 2009; Makuuchi et al., 2009), thereby subtracting away all those regions possibly activated for both simple and complex sentences. Area 45 (subdivided in the present analysis into receptor architectonical areas 45a and 45p; (Amunts et al., 2010) in the IFG has been shown to support semantic processes during sentence comprehension (Newman et al., 2010). Area 47 in the IFG has also been shown to be activated in language comprehension (Dronkers et al., 2004; Turken & Dronkers, 2011), and the clustering of the temporal area Te2 with pSTG/STS and the other language-related areas also correlates with its involvement in speech and language processing (Kubanek et al., 2013).

In the left hemisphere, the multimodal association areas of the IPL (PF, PFcm, PFm, PFop, PFt, PGa and PGp), superior parietal lobule (area 7), cingulate region (area 32), prefrontal cortex (areas 46 and 9), and ventral extrastriate cortex (areas FG1 and FG2) are clearly segregated from the primary sensory areas (V1, 3b and Te1), the hand representation region of the primary motor cortex (4d), and the language-related regions (labeled in red in Fig. 4). The discriminant analysis showed, that differences in M_1, α_1, and 5-HT_{1A} receptor densities contributed most, and in nicotinic α_4/β_2 and kainate receptors contributed least to the separation of areas 7, 9, 46, 32, FG1 and FG2 from the cluster containing the language-related areas. Segregation of the IPL areas was driven mainly by differences in the densities of $GABA_A$, α_2 and α_1 receptors. In the right hemisphere (Fig. S2), only the areas of the Broca region (44d, 44v, 45a, 45p and IFS1/IFJ) cluster together and are separated from the mouth motor representation area 4v, the prefrontal area 47 and the temporal areas pSTG/STS and Te2. This segregation was due mainly to differences in M_2, 5-HT_2 and NMDA receptor densities, and may reflect a difference between the language dominant left hemisphere and the right hemisphere.

Areas 7, 9, 46, 32, FG1 and FG2 build a separate cluster in the left hemisphere (Fig. 4) and have been demonstrated to be involved in a variety of cognitive functions. Although area 46 was described as being part of a language processing network (Turken & Dronkers, 2011), while area 9 was demonstrated to be involved in idiom comprehension (Romero, Walsh, & Papagno, 2006) and in fronto-temporal interactions for strategic inference processes during language comprehension (Chow, Kaup, Raabe, & Greenlee, 2008), both are also involved, as is area 7, in the neural network associated with working memory, planning, and reasoning-based decision making (D'Esposito, Postle, & Rypma, 2000; Levy & Goldman-Rakic, 2000; Marshuetz, Smith, Jonides, DeGutis, & Chenevert, 2000). Interestingly, deactivations of left areas 9 and 46 were found to correlate with activations of left area 32 during a task involving the processing of self-reflections during decision making (Deppe, Schwindt, Kugel, Plassmann, & Kenning, 2005). Although areas 46 and 9 are involved in language and memory processes, the fact that their receptor fingerprints build a cluster with those of other areas involved in memory functions (areas 7 and 32; Garn, Allen, & Larsen, 2009;

Hernandez, Martinez, & Kohnert, 2000; Kan & Thompson-Schill, 2004; Whitney et al., 2009) may highlight the preferential involvement of the prefrontal areas 46 and 9 in memory-related processes. The extrastriate visual areas FG1 and FG2 are associated with cognitive functions such as word form (left hemisphere) and face (right hemisphere) recognition, visual attention, and visual language perception (Caspers, Zilles, Amunts, et al., 2013; Dehaene & Cohen, 2011).

Although some of the IPL areas of the left hemisphere may belong to the functionally defined wider Wernicke region, they differ from 44v, 44d, 45a, 45p, IFS1/IFJ, and pSTG/STS in that they are not necessarily activated during sentence comprehension, but during semantic expectancy, preferentially in degraded speech (Obleser & Kotz, 2010; Obleser, Zimmermann, Van, & Rauschecker, 2007) and in semantic and phonological processing (Gernsbacher & Kaschak, 2003; Geschwind, 1970; Price, 2000). Furthermore, Obleser and Kotz (Obleser & Kotz, 2010) described these regions as "postsensory interface structure that taps long-term semantic knowledge/memory", and thus did not consider them to be directly involved in sentence comprehension. Area PFcm is comparable by its location and extent to area Spt, which supports auditory-motor integration for speech (Hickok et al., 2003). Although areas PFcm and pSTG/STS are assigned to different branches in the cluster tree (Fig. 4A), the multidimensional scaling analysis reveals that, out of the inferior parietal areas, the fingerprint of PFcm is the nearest neighbor of the pSTG/STS (Fig. 4B). This relationship could be caused by the fact that area Spt is known to be connected with the language area pSTG (Hickok and Poeppel 2007). The difference between the results of the hierarchical cluster tree and the multidimensional scaling analyses reflects different perspectives on the similarity criteria used for the analyses of multireceptor fingerprints. Whereas the hierarchical cluster analysis is based on a recursive algorithm which minimizes the total within cluster variance, the multidimensional scaling presents the best 2-dimensional representation of the distances between the fingerprints of the examined areas in a 15-dimensional (15 different receptors representing a fingerprint) space without applying any linkage between areas during the calculation process.

Concluding, the tight clustering of the receptor fingerprints of all language-related areas in the left hemisphere is impressive despite their cytoarchitectonical diversity and the fact that they are topographically widely distributed throughout the brain from the IFG to the posterior part of the superior temporal gyrus. The multireceptor fingerprint analysis provides the first evidence for a common molecular basis of interaction in the functionally defined sentence comprehension network. Cortical areas distinct by their multireceptor expression and defined by their function in encoding and decoding of words, and syntactically complex, verbal working memory demanding sentences interact in this network. Note, that on the basis of these data we are not claiming any language specificity of molecular fingerprints. We rather suggest that brain regions which work together in a functional network are characterized by a similarity in their fingerprints, which differ from those of other networks. Interestingly, we found a higher similarity of the receptor fingerprints in the frontal and temporal language regions extracted from the left, language dominant hemisphere, as compared to the right hemisphere.

Acknowledgments

This work was supported by grants of the European FET flagship project "Human Brain Project" (Subproject 2, Strategic Human Brain Data, WP2.1: Multi-level organisation of the human brain, T2.1.1: Distribution of receptors in the human cerebral cortex to K.Z. and K.A.), the Portfolio Theme "Supercomputing and Modeling for the Human Brain" of the Helmholtz Association, Germany (to K.A. and K.Z.), and the Doctoral Program of the Max Planck Institute for Human Cognitive and Brain Sciences (to M.B.-T.).

Supplementary data

Supplementary data related to this article can be found at http://dx.doi.org/10.1016/j.cortex.2014.07.007.

REFERENCES

Amunts, K., Lenzen, M., Friederici, A. D., Schleicher, A., Morosan, P., Palomero-Gallagher, N., et al. (2010). Broca's region: novel organizational principles and multiple receptor mapping. *PLoS Biology, 8*(9).

Amunts, K., Malikovic, A., Mohlberg, H., Schormann, T., & Zilles, K. (2000). Brodmann's areas 17 and 18 brought into stereotaxic space-where and how variable? *NeuroImage, 11*(1), 66–84.

Amunts, K., Schleicher, A., Bürgel, U., Mohlberg, H., Uylings, H. B. M., & Zilles, K. (1999). Broca's region revisited: cytoarchitecture and intersubject variability. *Journal of Comparative Neurology, 412*, 319–341.

Brodmann, K. (1909). *Vergleichende Lokalisationslehre der Großhirnrinde in ihren Prinzipien dargestellt auf Grund des Zellbaues* (Leipzig: Barth).

Caspers, S., Schleicher, A., Bacha-Trams, M., Palomero-Gallagher, N., Amunts, K., & Zilles, K. (2013a). Organization of the human inferior parietal lobule based on receptor architectonics. *Cerebral Cortex, 23*, 615–628.

Caspers, J., Zilles, K., Amunts, K., Laird, A. R., Fox, P. T., & Eickhoff, S. B. (2013b). Functional characterization and differential coactivation patterns of two cytoarchitectonic visual areas on the human posterior fusiform gyrus. *Human Brain Mapping*. http://dx.doi.org/10.1002/hbm.22364.

Caspers, J., Zilles, K., Eickhoff, S. B., Schleicher, A., Mohlberg, H., & Amunts, K. (2013c). Cytoarchitectonical analysis and probabilistic mapping of two extrastriate areas of the human posterior fusiform gyrus. *Brain Structure and Function, 218*(2), 511–526.

Caspers, S., Zilles, K., Laird, A. R., & Eickhoff, S. B. (2010). ALE meta-analysis of action observation and imitation in the human brain. *NeuroImage, 50*(3), 1148–1167.

Catani, M., Jones, D. K., & ffytche, D. H. (2005). Perisylvian language networks of the human brain. *Annals of Neurology, 57*(1), 8–16.

Chow, H. M., Kaup, B., Raabe, M., & Greenlee, M. W. (2008). Evidence of fronto-temporal interactions for strategic inference processes during language comprehension. *NeuroImage, 40*(2), 940–954.

Corbetta, M., Patel, G., & Shulman, G. L. (2008). The reorienting system of the human brain: from environment to theory of mind. *Neuron, 58*(3), 306–324.
Dehaene, S., & Cohen, L. (2011). The unique role of the visual word form area in reading. *Trends in Cognitive Sciences, 15*(6), 254–262.
Deppe, M., Schwindt, W., Kugel, H., Plassmann, H., & Kenning, P. (2005). Nonlinear responses within the medial prefrontal cortex reveal when specific implicit information influences economic decision making. *Journal of Neuroimaging, 15*(2), 171–182.
D'Esposito, M., Postle, B. R., & Rypma, B. (2000). Prefrontal cortical contributions to working memory: evidence from event-related fMRI studies. *Experimental Brain Research, 133*(1), 3–11.
Dronkers, N. F., Wilkins, D. P., Van Valin, R. D. J., Redfern, B. B., & Jaeger, J. J. (2004). Lesion analysis of the brain areas involved in language comprehension. *Cognition, 92*(1–2), 145–177.
Eickhoff, S. B., Rottschy, C., Kujovic, M., Palomero-Gallagher, N., & Zilles, K. (2008). Organizational principles of human visual cortex revealed by receptor mapping. *Cerebral Cortex, 18*(11), 2637–2645.
Eickhoff, S. B., Rottschy, C., & Zilles, K. (2007). Laminar distribution and co-distribution of neurotransmitter receptors in early human visual cortex. *Brain Structure and Function, 212*(3–4), 255–267.
Evans, A. C., Janke, A. L., Collins, D. L., & Baillet, S. (2012). Brain templates and atlases. *NeuroImage, 62*, 911–922.
Fiez, J. A. (1997). Phonology, semantics, and the role of the left inferior prefrontal cortex. *Human Brain Mapping, 5*(2), 79–83.
Formisano, E., De Martino, F., Bonte, M., & Goebel, R. (2008). "Who" is saying "what"? Brain-based decoding of human voice and speech. *Science, 322*(5903), 970–973.
Friederici, A. D. (2009). Pathways to language: fiber tracts in the human brain. *Trends in Cognitive Sciences, 13*(4), 175–181.
Friederici, A. D. (2011). The brain basis of language processing: from structure to function. *Physiological Reviews, 91*(4), 1357–1392.
Friederici, A. D., Fiebach, C. J., Schlesewsky, M., Bornkessel, I. D., & von Cramon, D. Y. (2006). Processing linguistic complexity and grammaticality in the left frontal cortex. *Cerebral Cortex, 16*(12), 1709–1717.
Friederici, A. D., Makuuchi, M., & Bahlmann, J. (2009). The role of the posterior superior temporal cortex in sentence comprehension. *NeuroReport, 20*(6), 563–568.
Garn, C. L., Allen, M. D., & Larsen, J. D. (2009). An fMRI study of sex differences in brain activation during object naming. *Cortex, 45*(5), 610–618.
George, M. S., Ketter, T. A., Parekh, P. I., Horwitz, B., Herscovitch, P., & Post, R. M. (1995). Brain activity during transient sadness and happiness in healthy women. *American Journal of Psychiatry, 152*, 341–351.
Gernsbacher, M. A., & Kaschak, M. P. (2003). Neuroimaging studies of language production and comprehension. *Annual Review of Psychology, 54*, 91–114.
Geschwind, N. (1970). The organization of language and the brain. *Science, 170*(3961), 940–944.
Geyer, S., Ledberg, A., Schleicher, A., Kinomura, S., Schormann, T., Bürgel, U., et al. (1996). Two different areas within the primary motor cortex of man. *Nature, 382*, 805–807.
Geyer, S., Schleicher, A., & Zilles, K. (1997). The somatosensory cortex of human: cytoarchitecture and regional distributions of receptor-binding sites. *NeuroImage, 6*, 27–45.
Grewe, T., Bornkessel, I., Zysset, S., Wiese, R., von Cramon, D. Y., & Schlesewsky, M. (2005). The emergence of the unmarked: a new perspective on the language-specific function of Broca's area. *Human Brain Mapping, 26*(3), 178–190.
Heim, S., Eickhoff, S. B., Ischebeck, A. K., Friederici, A. D., Stephan, K. E., & Amunts, K. (2009). Effective connectivity of the left BA 44, BA 45, and inferior temporal gyrus during lexical and phonological decisions identified with DCM. *Human Brain Mapping, 30*(2), 392–402.
Hernandez, A. E., Martinez, A., & Kohnert, K. (2000). In search of the language switch: an fMRI study of picture naming in Spanish-English bilinguals. *Brain and Language, 73*(3), 421–431.
Hickok, G., & Poeppel, D. (2007). The cortical organization of speech processing. *Nature Reviews Neuroscience, 8*, 393–402.
Hickok, G., Buchsbaum, B., Humphries, C., & Muftuler, T. (2003). Auditory–Motor Interaction Revealed by fMRI: Speech, Music, and Working Memory in Area Spt. *Journal of Cognitive Neuroscience, 15*(5), 673–682.
Jakobs, O., Wang, L. E., Dafotakis, M., Grefkes, C., Zilles, K., & Eickhoff, S. B. (2009). Effects of timing and movement uncertainty implicate the temporo-parietal junction in the prediction of forthcoming motor actions. *NeuroImage, 47*(2), 667–677.
Kan, I. P., & Thompson-Schill, S. L. (2004). Effect of name agreement on prefrontal activity during overt and covert picture naming. *Cognitive, Affective, & Behavioral Neuroscience, 4*(1), 43–57.
Keysers, C., & Gazzola, V. (2009). Expanding the mirror: vicarious activity for actions, emotions, and sensations. *Current Opinion in Neurobiology, 19*(6), 666–671.
Kross, E., Davidson, M., Weber, J., & Ochsner, K. (2009). Coping with emotions past: the neural bases of regulating affect associated with negative autobiographical memories. *Biological Psychiatry, 65*(5), 361–366.
Kubanek, J., Brunner, P., Gunduz, A., Poeppel, D., & Schalk, G. (2013). The tracking of speech envelope in the human cortex. *PLoS One, 8*(1), e53398.
Levy, R., & Goldman-Rakic, P. S. (2000). Segregation of working memory functions within the dorsolateral prefrontal cortex. *Experimental Brain Research, 133*(1), 23–32.
Makuuchi, M., Bahlmann, J., Anwander, A., & Friederici, A. D. (2009). Segregating the core computational faculty of human language from working memory. *Proceedings of the National Academy of Sciences of the United States of America, 106*(20), 8362–8367.
Marshuetz, C., Smith, E. E., Jonides, J., DeGutis, J., & Chenevert, T. L. (2000). Order information in working memory: fMRI evidence for parietal and prefrontal mechanisms. *Journal of Cognitive Neuroscience, 12*(Suppl. 2), 130–144.
Morosan, P., Schleicher, A., Amunts, K., & Zilles, K. (2005). Multimodal architectonic mapping of human superior temporal gyrus. *Anatomy and Embryology, 210*(5–6), 401–406.
Newman, S. D., Ikuta, T., & Burns, T., Jr. (2010). The effect of semantic relatedness on syntactic analysis: an fMRI study. *Brain and Language, 113*(2), 51–58.
Obleser, J., & Kotz, S. A. (2010). Expectancy constraints in degraded speech modulate the language comprehension network. *Cerebral Cortex, 20*(3), 633–640.
Obleser, J., Zimmermann, J., Van, M. J., & Rauschecker, J. P. (2007). Multiple stages of auditory speech perception reflected in event-related FMRI. *Cerebral Cortex, 17*(10), 2251–2257.
Palomero-Gallagher, N., Vogt, B. A., Schleicher, A., Mayberg, H. S., Schleicher, A., & Zilles, K. (2009). Receptor architecture of human cingulate cortex: evaluation of the four-region neurobiological model. *Human Brain Mapping, 30*(8), 2336–2355.
Price, C. J. (2000). The anatomy of language: contributions from functional neuroimaging. *Journal of Anatomy, 197*(Pt 3), 335–359.
Romero, L., Walsh, V., & Papagno, C. (2006). The neural correlates of phonological short-term memory: a repetitive transcranial magnetic stimulation study. *Journal of Cognitive Neuroscience, 18*(7), 1147–1155.
Saur, D., Kreher, B. W., Schnell, S., Kummerer, D., Kellmeyer, P., Vry, M. S., et al. (2008). Ventral and dorsal pathways for

language. *Proceedings of the National Academy of Sciences of the United States of America, 105*(46), 18035–18040.
Scheperjans, F., Palomero-Gallagher, N., Grefkes, C., Schleicher, A., & Zilles, K. (2005). Transmitter receptors reveal segregation of cortical areas in the human superior parietal cortex: relations to visual and somatosensory regions. *NeuroImage, 28*, 362–379.
Smith, R., Fadok, R. A., Purcell, M., Liu, S., Stonnington, C., Spetzler, R. F., et al. (2011). Localizing sadness activation within the subgenual cingulate in individuals: a novel functional MRI paradigm for detecting individual differences in the neural circuitry underlying depression. *Brain Imaging and Behavior, 5*(3), 229–239.
Thompson-Schill, S. L., D'Esposito, M., Aguirre, G. K., & Farah, M. J. (1997). Role of left inferior prefrontal cortex in retrieval of semantic knowledge: a reevaluation. *Proceedings of the National Academy of Sciences of the United States of America, 94*(26), 14792–14797.
Turken, A. U., & Dronkers, N. F. (2011). The neural architecture of the language comprehension network: converging evidence from lesion and connectivity analyses. *Frontiers in Systems Neuroscience, 5*, 1.
Upadhyay, J., Silver, A., Knaus, T. A., Lindgren, K. A., Ducros, M., Kim, D. S., et al. (2008). Effective and structural connectivity in the human auditory cortex. *Journal of Neuroscience, 28*(13), 3341–3349.
Vigneau, M., Beaucousin, V., Herve, P. Y., Duffau, H., Crivello, F., Houde, O., et al. (2006). Meta-analyzing left hemisphere language areas: phonology, semantics, and sentence processing. *NeuroImage, 30*(4), 1414–1432.
Whitney, C., Weis, S., Krings, T., Huber, W., Grossman, M., & Kircher, T. (2009). Task-dependent modulations of prefrontal and hippocampal activity during intrinsic word production. *Journal of Cognitive Neuroscience, 21*(4), 697–712.
Zilles, K., & Amunts, K. (2010). Centenary of Brodmann's map–conception and fate. *Nature Reviews Neuroscience, 11*(2), 139–145.
Zilles, K., Palomero-Gallagher, N., Grefkes, C., Scheperjans, F., Boy, C., Amunts, K., et al. (2002a). Architectonics of the human cerebral cortex and transmitter receptor fingerprints: reconciling functional neuroanatomy and neurochemistry. *European Neuropsychopharmacology, 12*, 587–599.
Zilles, K., Palomero-Gallagher, N., & Schleicher, A. (2004). Transmitter receptors and functional anatomy of the cerebral cortex. *Journal of Anatomy, 205*, 417–432.
Zilles, K., Schleicher, A., Palomero-Gallagher, N., & Amunts, K. (2002b). Quantitative analysis of cyto- and receptorarchitecture of the human brain. In A. W. Toga, & J. C. Mazziotta (Eds.), *Brain mapping. The methods* (2nd ed.). (pp. 573–602). Amsterdam: Elsevier.

Supplementary data

Figure S1: Receptor fingerprints of the examined brain regions in the right hemisphere.

Absolute densities (in fmol/mg protein) of 15 receptors shown as fingerprints of the examined brain regions. The positions of the different receptor types and the axis scaling are identical in all polar plots, and specified in the polar plot at the top left corner of the figure. The grey area represents the mean absolute receptor densities, SEM is given by the dashed lines.

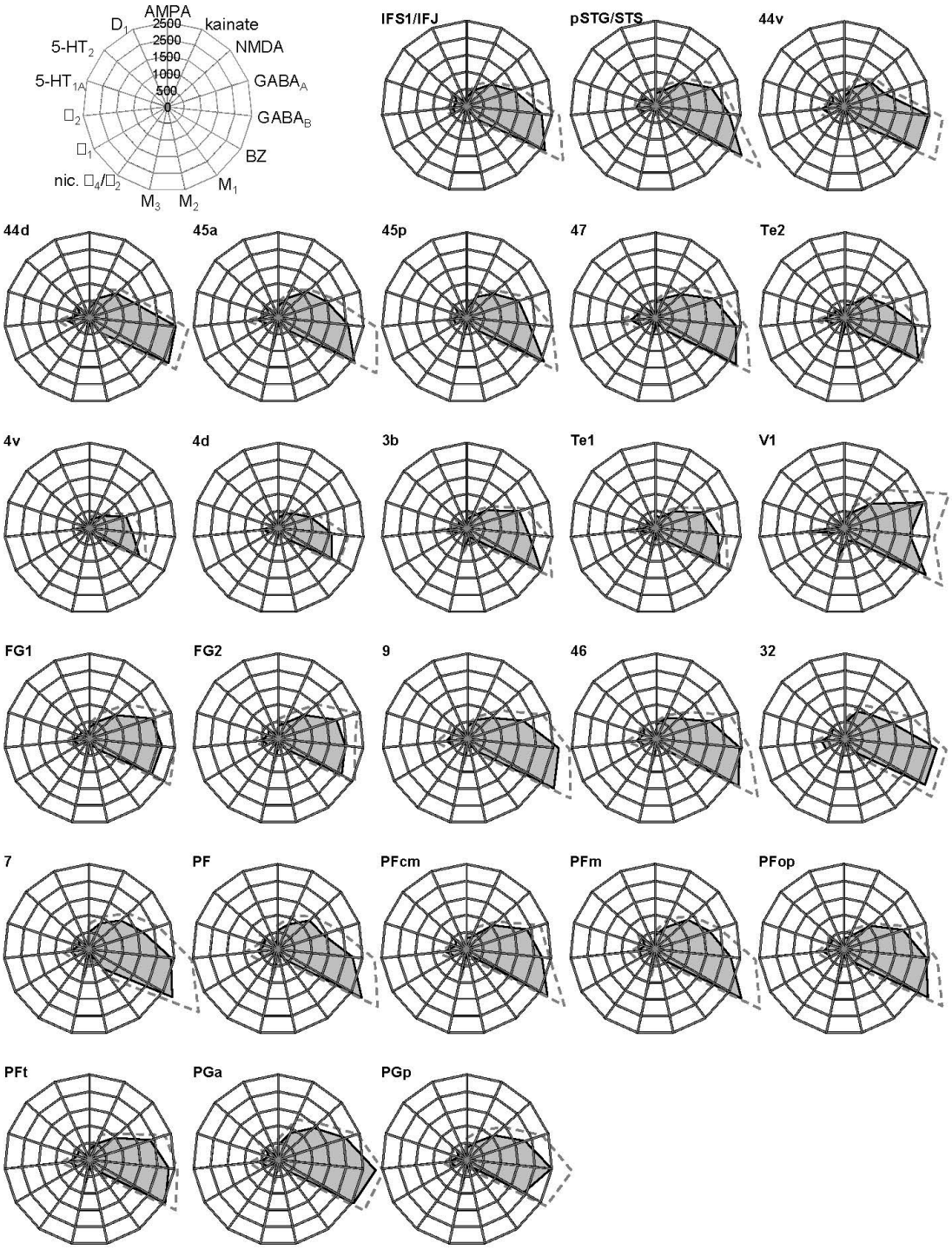

Figure S2: Hierarchical cluster tree and multidimensional scaling of receptor fingerprints in 26 cortical brain regions of the right hemisphere.

(**A**) Hierarchical cluster tree of receptor distribution patterns in the right hemisphere. (**B**) Multidimensional scaling resulting in a 2D display of the 15-dimensional receptor feature vectors of the receptor fingerprints of 26 cortical regions measured in the right hemisphere.

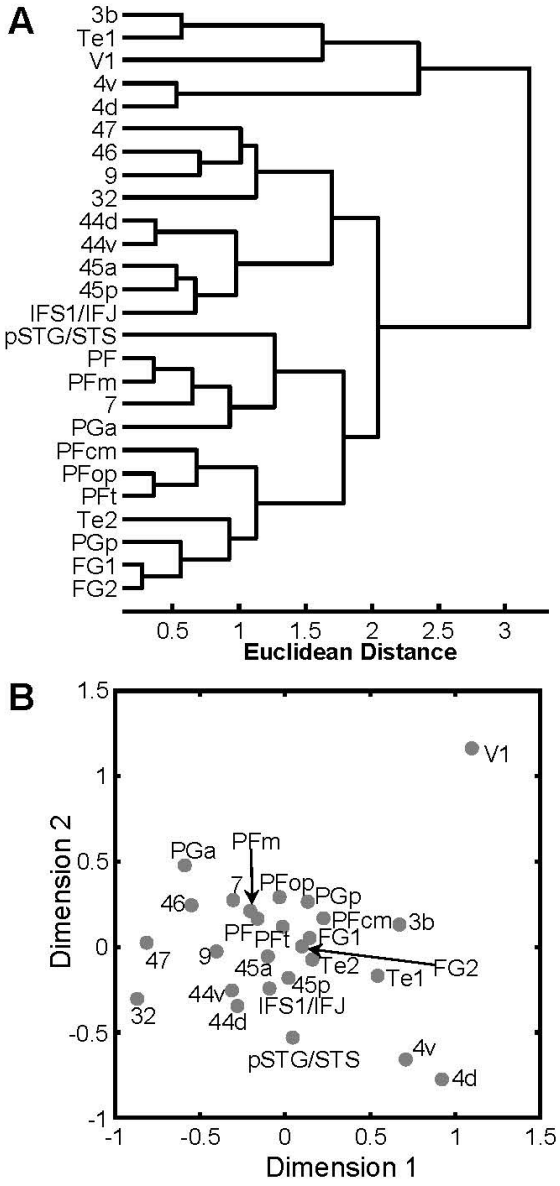

Supplementary Table 1: Binding protocols used for receptor autoradiography. Since the non-specific binding (measured after simultaneous incubation with the tritiated ligand and the respective displacer) was less than 5% for all receptors and cases, the total binding can be accepted as a measure of the specific binding. Substances listed between square brackets were only included in the buffer solution during the main incubation.

Transmitter	Receptor	Ligand	Displacer	Incubation buffer	Pre-incubation	Main incubation	Final rinsing
Glutamate	AMPA	[^{3}H]-AMPA (10.0 nM)	Quisqualate (10 µM)	50mM Tris-acetate (pH 7.2) [+ 100 mM KSCN]	3x10 min, 4ºC	45 min, 4ºC	1) 4x4sec, 4ºC 2) 2x2s Fixation
	kainate	[^{3}H]-Kainate (9.4 nM)	SYM 2081 (100 µM)	50mM Tris-acetate (pH 7.1) [+10 mM Ca^{2+}-acetate]	3x10 min, 4ºC	45 min, 4ºC	1) 3x4sec 2) Acetone glutaraldehyde (100 ml/2,5 ml), 2x2sec, 22ºC
	NMDA	[^{3}H]-MK-801 (3.3 nM)	(+)MK-801 (100 µM)	50mM Tris-acetate (pH 7.2) + 50 µM glutamate [+30 µM glycine + 50 µM spermidine]	15 min, 4ºC	60 min, 22 ºC	1) 2x5min, 4ºC 2) distilled water, 1x, 22ºC
GABA	$GABA_A$	[^{3}H]-Muscimol (7.7 nM)	GABA (10 µM)	50mM Tris-citrate (pH 7.0)	3x5 min, 4ºC	40 min, 4ºC	1) 3x3sec, 4ºC 2) distilled water, 1x, 22ºC
	$GABA_B$	[^{3}H]-CGP 54626 (2.0 nM)	CGP 55845 (100 µM)	50mM Tris-HCl (pH 7.2) + 2,5 mM $CaCl_2$	3x5 min, 4ºC	60 min, 4ºC	1) 3x2sec, 4ºC 2) distilled water, 1x, 22ºC
	BZ	[^{3}H]-Flumazenil (1.0 nM)	Clonazepam (2 µM)	170 mM Tris-HCl (pH 7.4)	15 min, 4ºC	60 min, 4ºC	1) 2x1min, 4ºC 2) distilled water, 1x, 22ºC
Serotonin	$5\text{-}HT_{1A}$	[^{3}H]-8-OH-DPAT (1.0 nM)	5-Hydroxy-tryptamine (1 µM)	170 mM Tris-HCl (p: 7.4) [+4 mM $CaCl_2$ + 0.01% ascorbate]	30 min, 22ºC	60 min, 22ºC	1) 5min, 4ºC 2) distilled water, 1x, 22ºC
	$5\text{-}HT_2$	[^{3}H]-Ketanserin (1.14 nM)	Mianserin (10 µM)	170 mM Tris-HCl (pH 7.7)	30 min, 22ºC	120 min, 22ºC	1) 2x10 min, 4ºC 2) distilled water, 1x, 22ºC
Acetylcholine	M_1	[^{3}H]-Pirenzepine (1.0 nM)	Pirenzepine (2 µM)	Modified Krebs buffer (pH 7.4)	15 min, 4ºC	60 min, 4ºC	1) 2x1min, 4ºC 2) distilled water, 1x, 22ºC
	M_2	[^{3}H]-Oxotremorine-M (1.7 nM)	Carbachol (10 µM)	20 mM HEPES-Tris (pH 7.5) + 10 mM $MgCl_2$ + 300 nM Pirenzepine	20 min, 22ºC	60 min, 22ºC	1) 2x2min, 4ºC 2) distilled water, 1x, 22ºC
	M_3	[^{3}H]-4-DAMP (1.0 nM)	Atropine sulfate (10 µM)	50 mM Tris-HCl (pH 7.4) + 0.1 mM PSMF + 1mM EDTA	15 min, 22ºC	45 min, 22ºC	1) 2x5min, 4ºC 2) distilled water, 1x, 22ºC
	Nic α_4/β_2	[^{3}H]-Epibatidine (0.5 nM)	Nicotine (100 µM)	15mM HEPES (pH 7.5) + 120 mM NaCl + 5.4 mM KCl + 0.8 mM $MgCl_2$ + 1.8 mM $CaCl_2$	20 min, 22ºC	90 min, 22ºC	1) 5min, 4ºC 2) distilled water, 1x, 22ºC
Noradrenaline	α_1	[^{3}H]-Prazosin (0.2 nM)	Phentolamine mesylate (10 µM)	50mM Na/K-phosphate buffer (pH: 7.4)	15 min, 22ºC	60 min, 22ºC	1) 2x5min, 4ºC 2) distilled water, 1x, 22ºC
	α_2	[^{3}H]-RX 821002 (1.4 nM)	Phentolamine mesylate (10 µM)	50 mM Tris-HCl + 100 µM $MnCl_2$ (pH: 7.7)	15 min, 22ºC	90 min, 22ºC	1) 5min, 4ºC 2) distilled water, 1x, 22ºC
Dopamine	D_1	[^{3}H]-SCH 23390 (1.67 nM)	SKF 83566 (1 µM)	50 mM Tris-HCl + 120 mM NaCl + 5 mM KCl + 2 mM $CaCl_2$ + 1 mM $MgCl_2$ (pH 7.4)	20 min, 22ºC	90 min, 22ºC	1) 2x20min, 4ºC 1x distilled water,, 22ºC